



Fluorescence emission and enhanced photochemical stability of Zn^{II}-5-triethyl ammonium methyl salicylidene ortho-phenylendiimine interacting with native DNA

Giampaolo Barone^{a,*}, Angela Ruggirello^b, Arturo Silvestri^{a,1}, Alessio Terenzi^a, Vincenzo Turco Liveri^b

^a Dipartimento di Chimica Inorganica e Analitica "S. Cannizzaro", Università di Palermo, Viale delle Scienze, Parco d'Orleans II, Edificio 17, 90128, Palermo, Italy

^b Dipartimento di Chimica Fisica "F. Accascina", Università di Palermo, Viale delle Scienze, Parco d'Orleans II, Edificio 17, 90128 Palermo, Italy

ARTICLE INFO

Article history:

Received 8 January 2010

Received in revised form 23 March 2010

Accepted 23 March 2010

Available online 31 March 2010

Keywords:

DNA

Fluorescence spectroscopy

Intercalation

Photooxidation

Schiff bases

Zinc

ABSTRACT

The photophysical and photochemical properties of the cationic Zn^{II} complex of 5-triethyl ammonium methyl salicylidene ortho-phenylendiimine (ZnL²⁺) interacting with native DNA were investigated by steady state and time-resolved fluorescence spectroscopies. Experimental results indicate that, in the presence of DNA, ZnL²⁺ is efficiently protected from a photochemical process, which occurs when it is in the free state dispersed in aqueous solution. The analysis of the absorption and emission spectra of ZnL²⁺, both stored in the dark and after exposure to tungsten lamp light for 24 h, corroborated by quantum chemical calculations, allowed us to point out that ZnL²⁺ undergoes a photoinduced two-electron oxidation process. According to this picture, the protective action of DNA toward the intercalated ZnL²⁺ was attributed to an effective inhibition of the ZnL²⁺ photooxidation. In this context, it can be considered that DNA-intercalated ZnL²⁺ is located in a region more hydrophobic than that sensed in the bulk water solvent. Moreover, by a thorough analysis of steady state and time-resolved fluorescence spectra, the interaction process can be consistently explained in terms of a complete intercalation of the complex molecules and that the polarity of the environment sensed by intercalated ZnL²⁺ is comprised between that of methanol and ethanol.

© 2010 Elsevier Inc. All rights reserved.

1. Introduction

Salen and Salphen, the di-anions of the Schiff bases N,N'-ethylenebis (salicylideneimine) and N,N'-phenylenebis (salicylideneimine), respectively, and ligands obtained by their chemical modifications, are of current interest for their potential and actual biomedical applications [1–13]. This is due to their peculiar molecular structure characterized by a nearly planar area with extended π system. Moreover, a wide class of complexes has been synthesized from these ligands that are able to coordinate metal ions via a square planar N₂O₂ system.

Among the various mechanisms through which they carry on their action in bioenvironments, of utmost importance is their direct interaction with DNA. Many DNA binding studies of metal complexes of Salen-type ligands have been reported in the literature, for example of Al [1], V [2], Mn [3–7], Fe [8,9], Co [6,10] Ni [2,5,6,11] Cu [2,6,12,13] and Zn [2]. The capability to interact with DNA is determined by several factors such as the nature of the ligand and the coordination geometry. Further necessary requisites that such complexes should obviously possess are to be stable and inert in biological environment

and water-soluble. Usually, water solubility has been increased by functionalizing the ligand by polar or charged groups [1–13].

Schiff base ligands and their metal complexes show interesting photophysical properties and display comparable fluorescence with excitation maxima at about 300 nm and emission maxima at about 420 nm [14]. For the ligand, fluorescence occurs through the proton transfer between the hydroxy and azomethine groups in the chromophore. Consequently, the polarity of the solvent has a marked effect [15]. Fluorescence emission from intraligand excited states of metal–Salen complexes has also been detected [16]. In particular, Zn (Salen) and related complexes are highly fluorescent [17] and their spectra are consistent with singlet emission in competition with efficient singlet-to-triplet intersystem crossing [18]. Concerning the photochemical properties of Zn^{II} complexes of Salen-type Schiff bases, these undergo a Zn^{II} mediated two-electron oxidation, due to simultaneous one-electron oxidation of the two keto-imine moieties of the bridging ligand. In fact, two redox processes at positive potential have been detected: the first oxidation process is likely localized on the phenolate ring of the Schiff base ligand while the second oxidation process may be a subsequent oxidation to form dicationic species [19]. Furthermore, in the presence of water, able to coordinate the Zn metal in the apical position, Zn(Salphen) complexes dissolved in relatively acidic organic solvents, such as CHCl₃, are known to lead to demetallated structures [20].

* Corresponding author. Tel.: +39 091427584; fax: +39 091590015.

E-mail addresses: gbarone@unipa.it (G. Barone), turco@unipa.it (V.T. Liveri).

¹ Professor Arturo Silvestri deceased on July 26th 2009.

The photophysical, photochemical and solution properties of Zn^{II} complexes recently reported [14–20] induced us to revisit the issue of stability of the Zn^{II} complex of 5-triethyl ammonium methyl salicylidene ortho-phenylendiimine (H_2L^{2+} , see Fig. 1) and further investigate the effect of light on ZnL^{2+} water solutions, also in the presence of native DNA. In fact, we have recently reported on the interaction of native DNA with NiL^{2+} , CuL^{2+} and ZnL^{2+} complexes [21,22], CuL^{2+} also confined in reverse micelles to simulate the intracellular solution environment [23]. The results obtained by UV spectrophotometric titrations, circular dichroism, DNA thermal denaturation measurements, and fluorescence quenching of ethidium bromide–DNA solutions, collectively show that ML^{2+} ($M = Ni^{II}$, Cu^{II} , and Zn^{II}) strongly interact with native DNA, by a combined electrostatic and intercalative mechanism [21,22]. Considering the photophysical properties of Zn^{II} –Schiff base complexes described above, fluorescence spectroscopy measurements were mainly exploited, as supported by quantum chemical calculations. In this way, we have extended our previous investigations of the DNA binding properties of ZnL^{2+} in aqueous solution, to achieve a detailed picture of the interaction mechanism and underlying phenomenology.

2. Materials and methods

The complex ZnL^{2+} was synthesized as recently reported [22] by the reaction of 5-(triethylammoniummethyl) salicylaldehyde chloride, 1,2 phenyldiamine and zinc(II) acetate in a 2:1:1 molar ratio [13], in doubly distilled water, and isolated as perchlorate salts. The 5-(triethylammoniummethyl) salicylaldehyde chloride ligand was prepared from 5-chloromethyl salicylaldehyde [24] and triethylamine in THF. The products were characterized by elemental analysis, UV and NMR spectroscopy, as reported [22]. 5-(triethylammoniummethyl) salicylaldehyde chloride (H_2LCl_2) 1H -NMR (300.13 MHz, D_2O , t, triplet; q, quartet; dd, double doublet, m, multiplet) δ (ppm): 1.33–1.38 (t, 9H, $J = 6.8$ Hz, CH_3); 3.11–3.23 (q, 6H, $J = 7.0$ Hz, CH_2); 4.41 (s, 2H, CH_2); 7.01–7.04 (d, 1H, $J = 9.5$ Hz, Ar); 7.59–7.64 (dd, 1H, $J = 2.5$ Hz, $J = 10.0$ Hz, Ar); 7.81–7.82 (d, 1H, $J = 2.5$ Hz, Ar); and 10.08 (s, 1H, CHO); the 1H -NMR spectrum of H_2LCl_2 exposed to tungsten lamp light for 24 h is practically identical to that of H_2LCl_2 stored in the dark. $ZnL(ClO_4)_2$ 1H -NMR (300.13 MHz, D_2O , sample stored in the dark) δ (ppm): 1.37 (t, 18H, CH_3 , $J = 7.0$ Hz); 3.20 (d, 12H, CH_2 , $J = 7.1$ Hz); 4.26 (s, 4H, CH_2); 6.90 (d, 2H, Ar, $J = 8.8$ Hz); 7.22–7.55 (m, 6H, Ar); 7.55–7.84 (m, 2H, Ar); and 8.88 (s, 2H, CH); the 1H -NMR spectrum of $ZnL(ClO_4)_2$ exposed to tungsten lamp light for 24 h is practically identical to that of $ZnL(ClO_4)_2$ stored in the dark. The NMR spectra were recorded on a Bruker Avance 300 spectrometer.

Lyophilized calf thymus DNA (Fluka, BioChemika) was resuspended in 1.0×10^{-3} M tris-hydroxymethyl-aminomethane (Tris-HCl) pH 7.5 and dialyzed as described in the literature [25]. DNA concentration, expressed in monomers units ($[DNA_{phosphate}]$), was determined by UV spectrophotometry using the molar absorption coefficient $7000 M^{-1} cm^{-1}$ at 258 nm [26]. All experiments were carried in Tris-HCl aqueous buffer at pH 7.5. Samples at fixed ZnL^{2+} concentration ($[ZnL^{2+}] = 5 \times 10^{-5}$ M) and various R values ($R = [DNA_{phosphate}]/[ZnL^{2+}]$) were prepared by

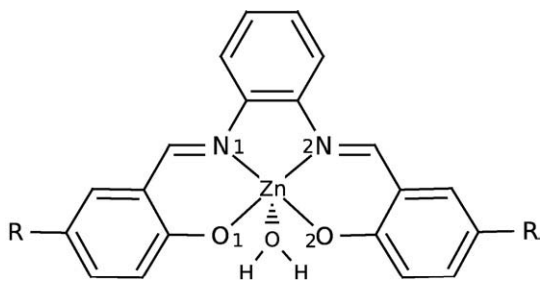


Fig. 1. Structure of the pentacoordinated aquo-complexes $ZnL \cdot H_2O^{2+}$ ($H_2L^{2+} = 5$ -triethyl ammonium methyl salicylidene ortho-phenylendiimine, $R = CH_2NEt_3^+$) and $ZnL' \cdot H_2O$ ($H_2L' = N,N'$ -phenylene-bis(salicylideneimine), $R = H$).

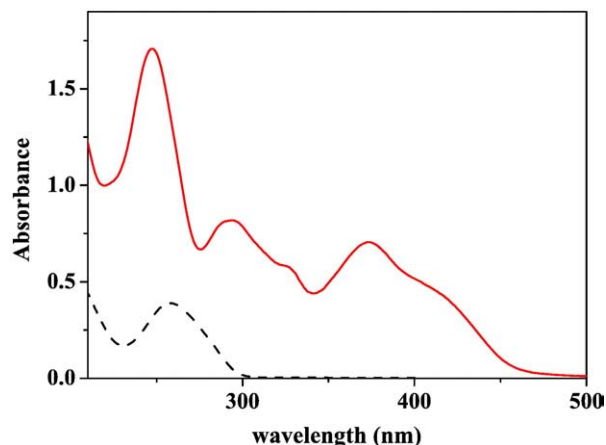


Fig. 2. Absorption spectra of buffered aqueous solutions of DNA, $[DNA_{phosphate}] = 5 \times 10^{-5}$ M, (---) and of ZnL^{2+} , $[ZnL^{2+}] = 5 \times 10^{-5}$ M, (—).

mixing the aqueous stock solutions of ZnL^{2+} ($[ZnL^{2+}] = 1 \times 10^{-4}$ M) and DNA ($[DNA_{phosphate}] = 1.31 \times 10^{-2}$ M).

UV-visible (UV-vis) spectra were recorded at 25 °C in the wavelength range 200–800 nm on a Perkin-Elmer (Lambda-900) spectrometer using Suprasil quartz cells with 10 mm optical path length. Steady-state fluorescence measurements were recorded at 25 °C in the wavelength range 360–700 nm on a Horiba Jobin Yvon spectrofluorimeter (Fluoromax-4) with excitation at 370 nm and arranged in T-shaped geometry. Time-correlated single photon counting (TCSPC) measurements were carried out using the Fluoromax-4 apparatus equipped with a Single Photon Counting Controller (FluoroHub, Horiba Jobin Yvon) and a pulsed diode light source (Nanoled, repetition rate 1 MHz, pulse duration 1.27 ns, 368 nm); data fitting was accomplished using least-squares methods with DAS6 Fluorescence Decay Analysis Software. All spectra were made using a 10 mm path length cuvette and were corrected for buffer fluorescence.

3. Theoretical calculations

The geometry of the H_2L^{2+} Schiff base ligand and of ZnL^{2+} ground states, both the square planar and the pentacoordinated aquo-complexes [27] (Fig. 1), as well as those of their mono and dioxidized forms, was fully optimized by the spin unrestricted Density Functional Theory (DFT) B3LYP method [28], using the all-electron double-zeta split-valence plus polarization (DZVP) basis set [29,30]. The spin state of the considered species was singlet (S0) for the lowest oxidation state, doublet (D0) for the monooxidized form and both singlet (S0) and triplet (T0) spin states for the dioxidized forms, respectively. Their absorption spectra were calculated by the Time Dependent DFT (TD-DFT) method [31–34], by using the same functional and basis set described above. To evaluate the emission spectra of the ZnL^{2+} aquo-complexes, in the reduced and dioxidized forms, TD-DFT calculations were performed on the first singlet excited states (S1) of the Zn^{II} (Salphen) simplified model complex, ZnL' (Fig. 1, $H_2L' = N,N'$ -phenylene-bis(salicylideneimine)), obtained by substitution of the two triethyl ammonium methyl cationic groups by two hydrogen atoms, whose geometry was optimized by the Configuration Interaction Singles (CIS) method [35,36] and using the DZVP basis set. Although it is known that the accuracy of the CIS method is comparable to that of the Hartree-Fock method for the ground state [37], nevertheless the main structural differences between the ground and first excited states are consistently reproduced by the CIS approach [38]. Implicit solvent effects in the electronic transitions were considered by single point calculations within the conductor-like polarized continuum model [39]. All calculations were performed using the Gaussian03 program package [40]. The calculated

absorption and emission electronic spectra were reproduced by the help of the GaussSum-2.1.6 program package [41].

4. Results and discussion

4.1. Photochemical behavior of ZnL^{2+} and protective effect of DNA

Preliminary experiments were carried out to ascertain the feasibility of the spectrofluorimetric investigation of the photophysical and photochemical properties of ZnL^{2+} intercalated in native calf thymus DNA. First of all, the absorption spectra of a buffered aqueous solution of DNA ($[DNA_{\text{phosphate}}] = 5 \times 10^{-5}$ M) and of ZnL^{2+} ($[ZnL^{2+}] = 5 \times 10^{-5}$ M) were collected to select the best suited excitation wavelength. Such spectra are shown in Fig. 2. Since the complex shows an absorption band centered at about 370 nm in a region where DNA does not absorb, we selected this excitation wavelength for our fluorescence experiments.

After detecting a fluorescence band in the 360–700 nm region, suitable experimental conditions and apparatus set up were searched,

allowing us to collect the fluorescence spectra without significant sample photodegradation.

It was found that, using the excitation wavelength of 370 nm, an entrance slit width of 0.24 mm and a scan rate of 6 nm/s nearly identical replicate spectra were collected. Furthermore, in order to evaluate the photochemical stability of ZnL^{2+} , the fluorescence spectra of some selected samples at various R values ($R = [DNA_{\text{phosphate}}]/[ZnL^{2+}]$) were collected at $t = 0$ h (freshly prepared samples) and after 24 h by maintaining the samples at room temperature i) in the dark or ii) under the illumination of a tungsten lamp (100 watt) placed at a fixed distance of 30 cm from the quartz cuvette (10 mm path length) containing the sample. The comparison among these spectra is shown in Fig. 3. It can be noted that, after 24 h, all the samples maintained in the dark are only marginally affected. On the other hand, while the sample at $R = 0$ after illumination displays a marked enhancement of its fluorescence intensity, by increasing the amount of DNA this effect progressively disappears being negligible at $R \geq 5$. Taking into account that ZnL^{2+} is intercalated within the DNA structure [22], quite surprisingly this

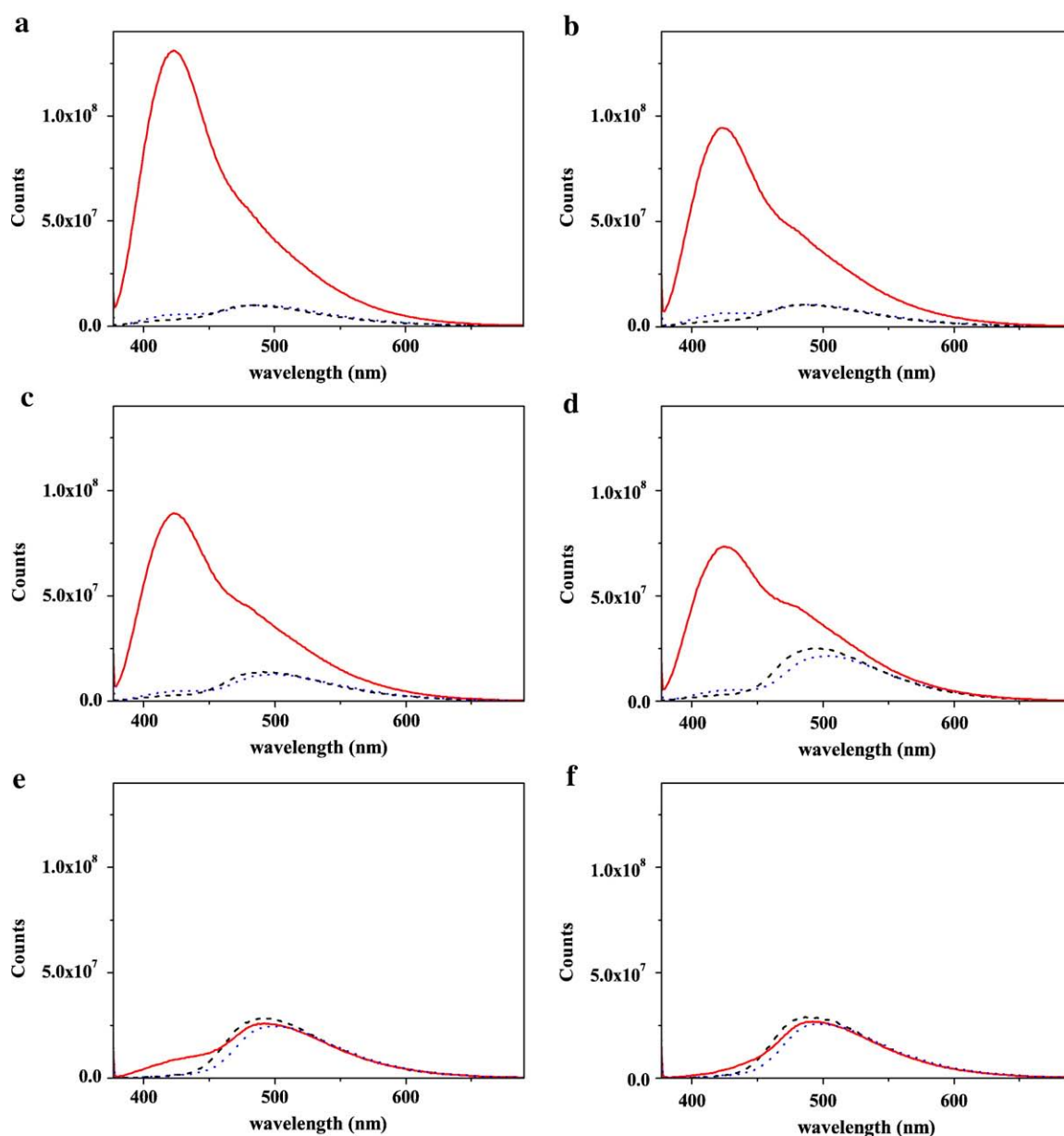


Fig. 3. Fluorescence spectra of samples at fixed ZnL^{2+} concentration, $[ZnL^{2+}] = 5 \times 10^{-5}$ M, and various R values: a, $R = 0$; b, $R = 0.2$; c, $R = 0.8$; d, $R = 2.0$; e, $R = 5.0$; f, $R = 10.0$, for $t = 0$ h (---), stored in the dark for $t = 24$ h (· · ·) and exposed to tungsten lamp light for $t = 24$ h (—).

finding indicates that the insertion of the Zn^{II} complex in the DNA double helix involves an efficient protection against the observed photochemical process. Moreover, it emphasizes a novel and interesting functionality of the DNA molecules which could be exploited for biomedical applications. In fact, being ZnL^{2+} representative of potentially interesting DNA-intercalating drugs, our finding could suggest the formulation of photounstable drugs that become photostable after DNA intercalation. Therefore, it should be of utmost interest to speculate i) on the nature of this photochemical process and ii) on the ability of the DNA double helix to hinder it.

Measurements performed at different light exposition times show that the fluorescence intensity of the ZnL^{2+} solutions exposed to light has a drastic enhancement within the first 24 h. After this period, further exposition to light negligibly changes both the fluorescence intensity and the band shape. Moreover, the fluorescence spectra of the samples stored in the dark for several days, after prolonged light exposition, are essentially coincident with those registered immediately after light exposition. These results allow us to conclude that: 1) the photoproduct is stable and 2) the process is irreversible. Interestingly, the same dramatic intensity enhancement was observed, after exposure to tungsten light for 24 h, for deoxygenated solutions of the ZnL^{2+} complex in Tris-HCl 1 mM. The latter were obtained by extensively insufflating nitrogen gas in the solvent and keeping it under nitrogen atmosphere.

The striking increase in the fluorescence quantum yield of the illuminated ZnL^{2+} in the free state strongly suggests the occurrence of a photochemical process resulting in an increase of the structural rigidity of the zinc(II) complex that remarkably reduces the radiationless decay rate from the excited to the ground state [42]. An additional support to this hypothesis comes from the light sensitivity observed in a Co^{II} -Salen-type complex, that is irreversibly photooxidized to a cationic species, and in which the electron is not removed from the metal but from the ligand [43]. Moreover, it has been reported that a Mn^{III} complex of a Salen-type ligand in $CHCl_3$ is photooxidized to a Mn^{IV} complex although, in addition, secondary processes can lead to various photoproducts [44]. Concerning the latter remark, it is known that visible light promotes the oxidation of the ligand in a Mn^{III} Salen-type complex, followed by the hydrolysis and rearrangement of the coordinated Schiff base ligand [45].

According to these considerations and recalling the results by Germain et al. [19], proving that Salen-type Schiff bases may undergo a Zn^{II} mediated two-electron oxidation, we attempted to rationalize our experimental findings in terms of the photooxidation of the ZnL^{2+} complex, by comparing experimental spectra with those obtained through TD-DFT calculations.

It is well known that, in aqueous solutions at neutral pH, any kind of native DNA, independently from its chain length distribution and base pair composition is characterized by the same surface charge density [46]. It is then reasonable to expect that also native DNA from any other source than from calf thymus should play the same protective effect against ZnL^{2+} photooxidation.

It should also be noted that the fluorescence spectrum of aqueous H_2L^{2+} Schiff base ligand is also somewhat influenced by light exposure but, remarkably, it is strongly different from that of the illuminated ZnL^{2+} sample at $R=0$ (see Fig. 4).

This leads us to exclude that the observed photochemical process consists in the complex demetallation. An explanation of the latter evidence may be given by considering that bulk water is known to be a base less strong than water traces dissolved in apolar solvents (or in relatively acidic solvents such as $CHCl_3$). Moreover, the presence of the Tris-HCl buffer at neutral pH may enhance the stability of the ZnL^{2+} complex towards demetallation [20].

To further investigate photochemical stability in water solutions of ZnL^{2+} , 1H -NMR spectra were recorded in D_2O for samples stored in the dark and exposed to tungsten lamp light for 24 h (see Fig. 5).

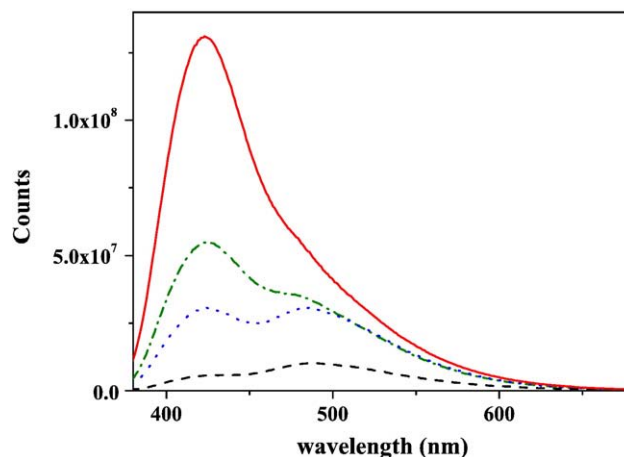


Fig. 4. Fluorescence spectra of aqueous solutions of ZnL^{2+} and H_2L^{2+} , $[ZnL^{2+}] = [H_2L^{2+}] = 5 \times 10^{-5}$ M, stored in the dark (ZnL^{2+} - - -, H_2L^{2+} ···) and exposed to tungsten lamp light for 24 h (ZnL^{2+} —, H_2L^{2+} - · -).

Remarkably, the 1H -NMR spectrum of ZnL^{2+} exposed to light shows the same peaks of the sample stored in the dark. Considering that the photooxidation of the ZnL^{2+} complex does not modify significantly its structure, these findings are consistent with the hypothesis that light exposure causes partial photooxidation of the ZnL^{2+} complex.

4.2. Comparison between experimental and calculated absorption and emission spectra of ZnL^{2+} and ZnL'

The absorption spectra of the H_2L^{2+} ligand, of the ZnL^{2+} tetracoordinated complex (Fig. 1) and of the $ZnL^{2+} \cdot H_2O$ pentacoordinated complex (Fig. 1) were calculated by the TD-DFT method, in the spin states S0 for the lowest oxidation state, D0 for the monooxidized form and S0 and T0 for the dioxidized forms.

The comparison between calculated and experimental absorption spectra shown in Fig. 6, induced us to consider that in water solution ZnL^{2+} should be coordinated by an axial water molecule and the presence of square planar ZnL^{2+} and/or of the H_2L^{2+} ligand can be safely excluded. In fact, there is a better matching between the experimental absorption spectrum of ZnL^{2+} , stored in the dark (Fig. 6d), and that calculated for $ZnL^{2+} \cdot H_2O$ in the singlet spin ground state (Fig. 6b, see also Fig. 7 dashed lines).

The latter conclusion is better illustrated by Fig. 7, where the absorption spectrum of $ZnL^{2+} \cdot H_2O$ S0 and the average of the two spectra corresponding to the reduced $ZnL^{2+} \cdot H_2O$ S0 and dioxidized $ZnL^{2+} \cdot H_2O$ T0 state are reported in Fig. 7b. In particular, the similarity between the calculated absorption spectrum obtained by a 50% mixture of the S0 $ZnL^{2+} \cdot H_2O$ and T0 $ZnL^{4+} \cdot H_2O$ with experimental absorption spectrum of illuminated ZnL^{2+} in water solution, supports the hypothesis that the effect of the tungsten lamp light for 24 h is to partially oxidize ZnL^{2+} to ZnL^{4+} , up to an approximately equimolar ratio between the two forms. To understand the role of light exposure on the fluorescence emission of ZnL^{2+} water solutions, we have calculated the structure of the first excited state of simplified model complexes $ZnL' \cdot H_2O$ and $ZnL'^{2+} \cdot H_2O$ (see Fig. 1) by the CIS method, in the S1 spin states for both the reduced and the dioxidized states (see Theoretical calculations section). Their emission spectra calculated by the TD-DFT method are shown in Fig. 8. Despite the remarkable difference between the experimental fluorescence intensities of ZnL^{2+} solutions stored in the dark and illuminated, due to their different nonradiative decay rates, the shape of the calculated emission spectra in Fig. 8 nicely reproduces the spectral changes accompanying the exposure to light. In fact, in the experimental spectrum (Fig. 8a) the peak at 420 nm is red shifted in the illuminated

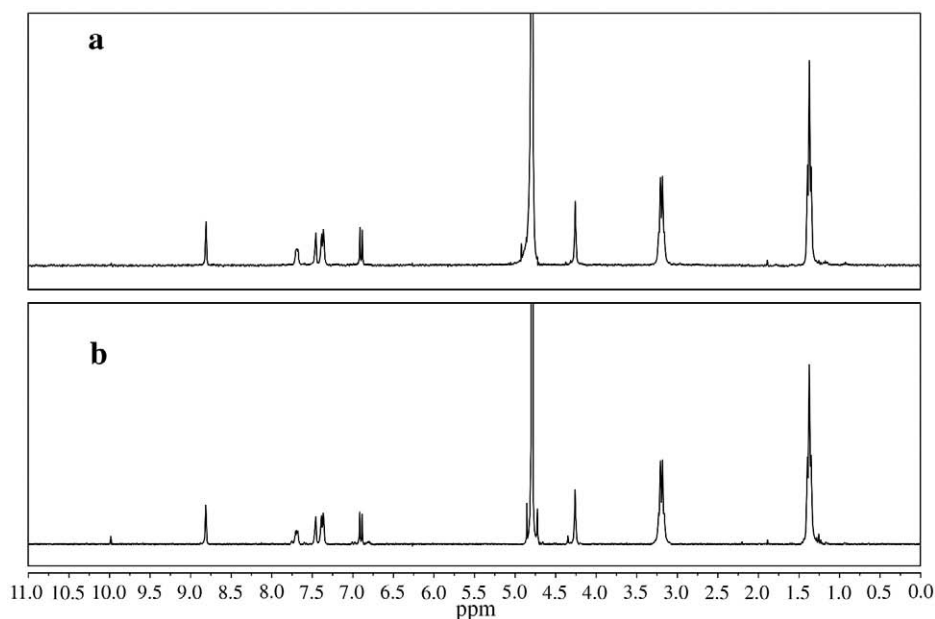


Fig. 5. $^1\text{H-NMR}$ spectra of $\text{ZnL}(\text{ClO}_4)_2$ in D_2O , stored in the dark (a) and exposed to tungsten lamp light for 24 h (b).

ZnL^{2+} solutions and the intensity of the peak at 480 nm decreases compared to that at 420 nm. Moreover, the analysis of Figs. 6 and 8 shows that the ground state of the dioxidized ZnL^{4+} aquo-complex

is a triplet spin state, while the emission from the first excited state of the dioxidized species occurs from the S_1 singlet spin state, presumably following a triplet to singlet intersystem crossing.

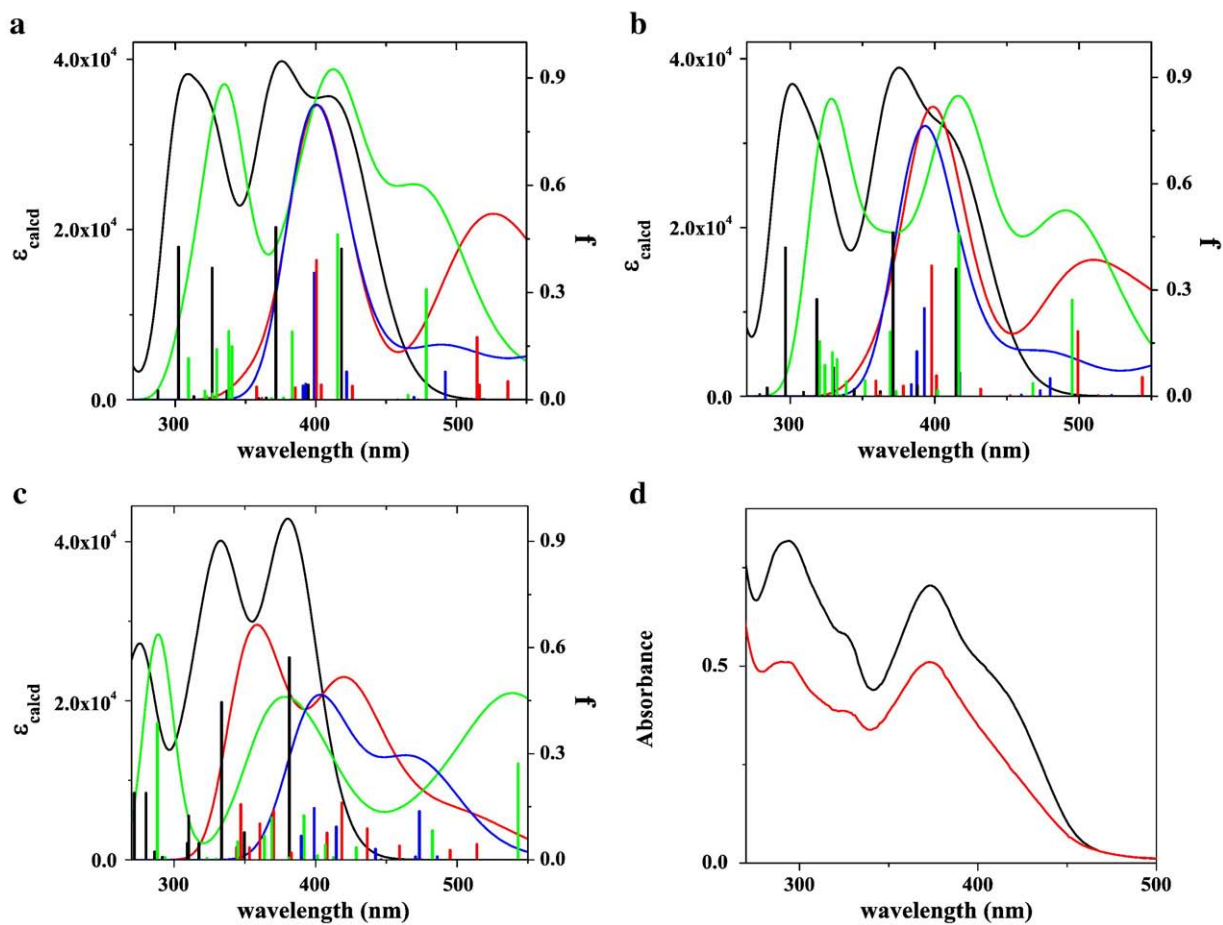


Fig. 6. Calculated absorption spectra (ϵ_{calc}) and oscillator strengths (f) of ZnL^{2+} (a), $\text{ZnL}^{2+} \cdot \text{H}_2\text{O}$ (b) and H_2L^{2+} (c) in the reduced S_0 state (—), in its monooxidized D_0 state (—) and in the dioxidized S_0 (—) and T_0 (—) spin states, within the implicit water solvent; (d) experimental absorption spectra of ZnL^{2+} ($[\text{Zn}^{2+}] = 5 \times 10^{-5} \text{ M}$), stored in the dark (—) and exposed to the tungsten lamp light for 24 h (—).

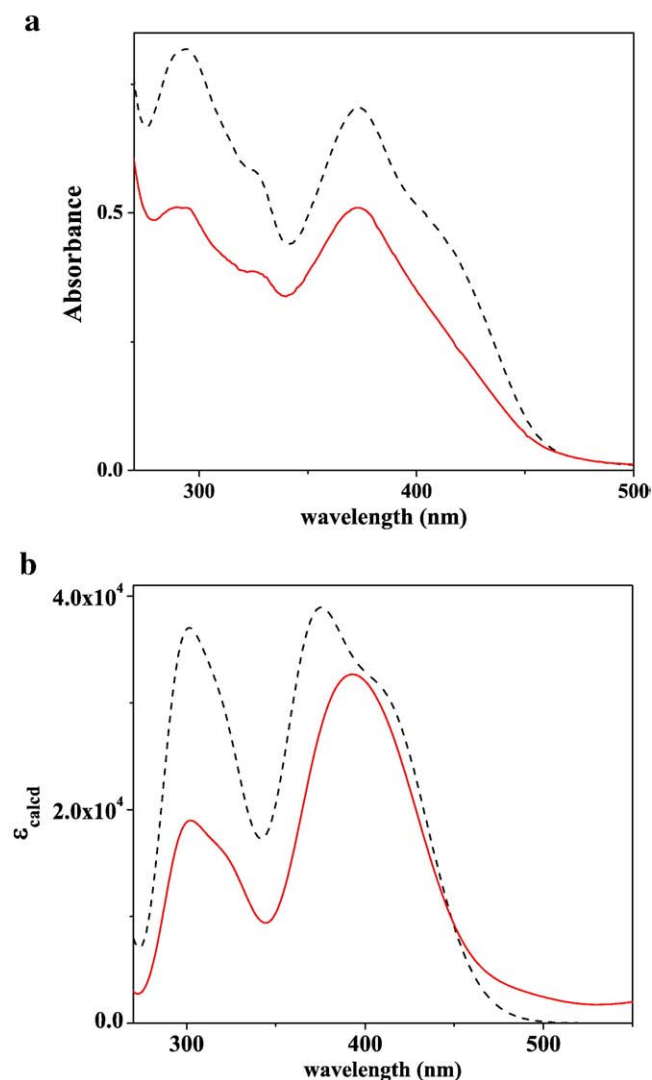


Fig. 7. Experimental absorption spectra of ZnL^{2+} (a) and calculated spectra of $\text{ZnL}^{2+} \cdot \text{H}_2\text{O}$ within the implicit water solvent (b): (a) experimental ($[\text{ZnL}^{2+}] = 5 \times 10^{-5} \text{ M}$), stored in the dark (---) and exposed to the tungsten lamp light for 24 hours (—); (b) reduced S0 state (---) and 50% mixture of the reduced S0 state and dioxidized T0 state (—).

Noteworthy, the increase in the positive charge accompanying the two-electron oxidation process, may well explain the increase of the photoinduced structural rigidity of the cationic zinc(II) complex, as deduced above from the analysis of the experimental spectra (see Fig. 3a). The most intense electronic transitions of the absorption spectra calculated for $\text{ZnL}^{2+} \cdot \text{H}_2\text{O}$ S0 and for $\text{ZnL}^{4+} \cdot \text{H}_2\text{O}$ T0 (see Fig. 6b) and of the emission spectra calculated for $\text{ZnL}' \cdot \text{H}_2\text{O}$ S1 and for $\text{ZnL}^{2+} \cdot \text{H}_2\text{O}$ S1 (see Fig. 8b), can be attributed to electronic transitions among the Molecular Orbitals (MOs) depicted in Fig. 9, as detailed in Table 1.

Interestingly, it can be noticed that the contribution of the orbitals centered on the metal ion is negligible in all the MOs represented Fig. 9. This result shows that the calculated electronic transitions, of both the absorption and emission spectra, involve intraligand states, in agreement with the attributions reported in the literature [16].

Another interesting finding concerns the similarity between the MOs involved in the absorption and emission electronic transitions. For example, the shape of the Highest Occupied Molecular Orbital (HOMO), HOMO-4, Lowest Unoccupied Molecular Orbital (LUMO) and LUMO+1 orbitals calculated for $\text{ZnL}^{2+} \cdot \text{H}_2\text{O}$ essentially coincide with that of the HOMO, HOMO-1, LUMO and LUMO+1 orbitals calculated for $\text{ZnL}' \cdot \text{H}_2\text{O}$. On the other hand, being $\text{ZnL}^{4+} \cdot \text{H}_2\text{O}$ in the

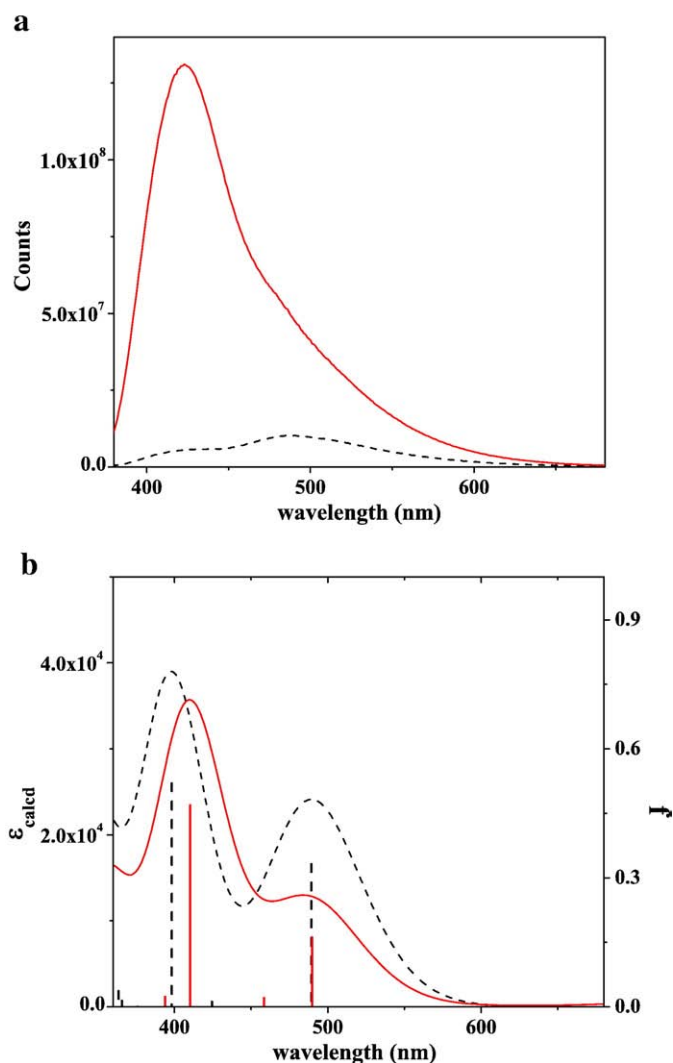


Fig. 8. (a) Experimental fluorescence spectra of ZnL^{2+} , $[\text{ZnL}^{2+}] = 5 \times 10^{-5} \text{ M}$, stored in the dark (---) and exposed to the tungsten lamp light for 24 h (—); (b) calculated emission spectra (ϵ_{calc}) and oscillator strengths (f) for the simplified $\text{ZnL}' \cdot \text{H}_2\text{O}$ complex, within the implicit water solvent, reduced S1 state (---) and dioxidized S1 state species (—).

triplet spin state and $\text{ZnL}^{2+} \cdot \text{H}_2\text{O}$ in the singlet spin state, the shape of the HOMO and LUMO of $\text{ZnL}^{4+} \cdot \text{H}_2\text{O}$ is comparable to that of the LUMO and LUMO+1 of $\text{ZnL}^{2+} \cdot \text{H}_2\text{O}$. Finally, it is worth considering that the triethyl ammonium methyl groups are essentially not involved in the MOs of both $\text{ZnL}^{2+} \cdot \text{H}_2\text{O}$ and $\text{ZnL}^{4+} \cdot \text{H}_2\text{O}$ shown in Fig. 9. This suggests that $\text{ZnL}' \cdot \text{H}_2\text{O}$ is a reliable model for describing the excited state of $\text{ZnL}^{2+} \cdot \text{H}_2\text{O}$. Table 2 shows the relevant bond lengths and angles involving the oxygen and nitrogen atoms coordinated to the Zn atom in the four metal complexes $\text{ZnL}^{2+} \cdot \text{H}_2\text{O}$, $\text{ZnL}^{4+} \cdot \text{H}_2\text{O}$, $\text{ZnL}' \cdot \text{H}_2\text{O}$ and $\text{ZnL}^{2+} \cdot \text{H}_2\text{O}$. The geometry of the first singlet excited state of the reduced and oxidized forms of the Zn^{II} complex has been obtained on a simplified system (see Fig. 1) and using the CIS method. The latter is less accurate than the B3LYP method used for the description of the reduced and oxidized forms in the ground state. Nevertheless the analysis of Table 2 suggests that only minor structural modifications occur on the coordination site of the title complex when it is photooxidized and/or when it is photoexcited. However, interestingly, such small distortions largely take into account of the remarkable spectral differences, experimentally detected both in the absorption and in the emission electronic transitions (see Figs. 6 and 8).

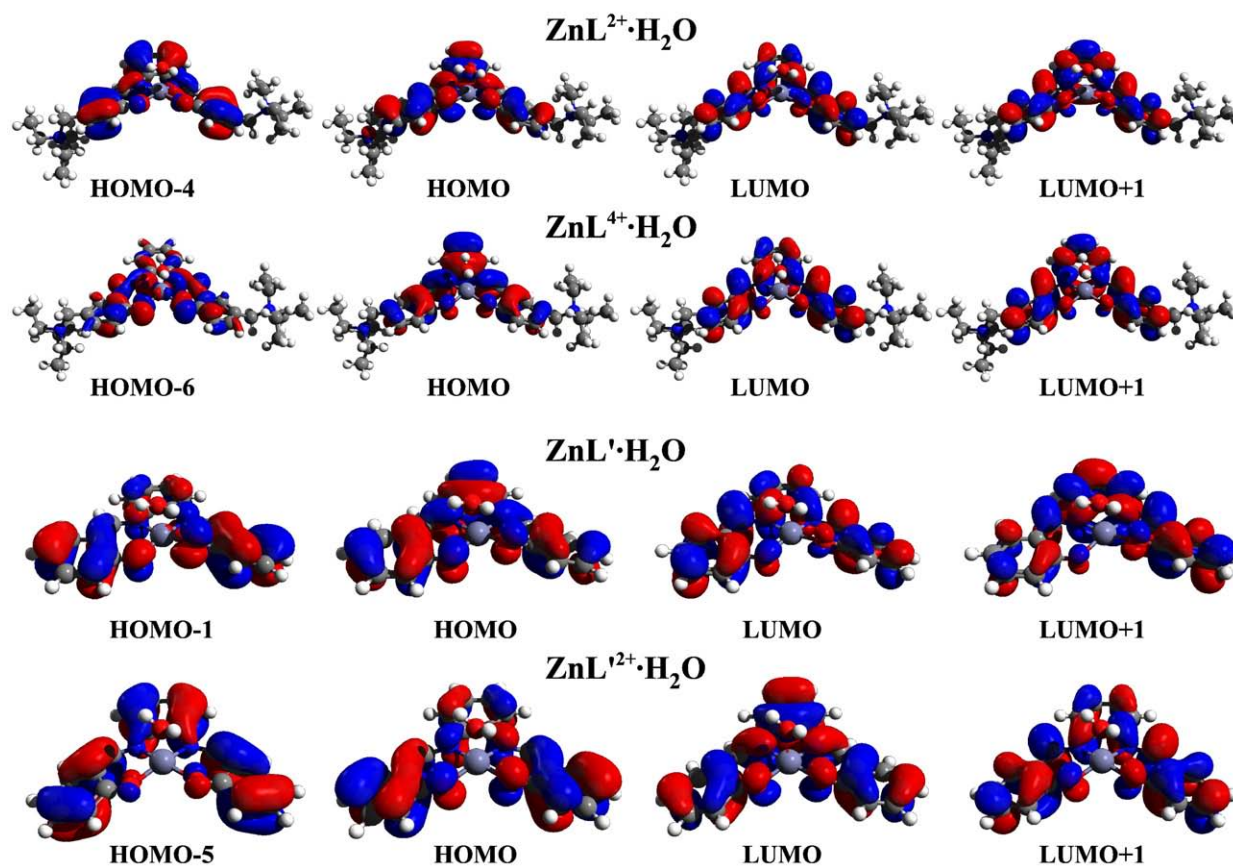


Fig. 9. Molecular orbitals involved in the electronic transitions calculated for the absorption spectra of the $\text{ZnL}^{2+} \cdot \text{H}_2\text{O}$ S0 and of the dioxidized $\text{ZnL}^{4+} \cdot \text{H}_2\text{O}$ T0 (top rows), and for the emission spectra of the corresponding simplified models, $\text{ZnL}' \cdot \text{H}_2\text{O}$ S1 and $\text{ZnL}'^{2+} \cdot \text{H}_2\text{O}$ S1 excited states (bottom rows).

According to this picture, the protective action of DNA toward the intercalated ZnL^{2+} can be attributed to the inhibition of the ZnL^{2+} photooxidation through an effective stabilization of its ground S0 state (see Fig. 3). The occurrence of ZnL^{2+} photooxidation in bulk water solution induces to hypothesize that an electron transfer takes place from each of the salicylideneimine groups to a water molecule. It is worth in fact recalling that the same photooxidation process also occurs in deoxygenated solutions (see above). Hence, a possible explanation of the way by which DNA hinders this process and protects ZnL^{2+} from the photooxidation, can be given considering that the DNA-intercalated ZnL^{2+} compound is in a more hydrophobic region, less accessible to water molecules (see below). Then, in agreement with the above reported findings, to investigate the photophysical properties of intercalated ZnL^{2+} , all the subsequent

fluorescence experiments were carried out using samples prepared and stored in the dark before each measurement.

4.3. Steady-state and time-resolved photophysical properties of ZnL^{2+} intercalated in native DNA

Under excitation at 370 nm, ZnL^{2+} aqueous solutions show an intense structured emission band centered at 483 nm, whose intensity increases in the presence of DNA. The increase of the fluorescence intensity is accompanied by a red-shift of the fluorescence maximum (see Fig. 10). These findings are typical clues of the occurrence of an intercalation process and in particular indicates that in the intercalated state the complex probes either (i) an environment less polar than water or (ii) a restriction of molecular motions or (iii) solvent relaxation that deactivates the excited state without emission of a photon [47]. In particular, by adding increasing amounts of DNA at fixed complex

Table 1

Attribution of the most intense calculated absorption and emission transitions of the considered Zn^{II} complexes (see Figs. 6b and 8b) to the frontier molecular orbitals essentially involved (see Fig. 9).

Compound	λ (nm)	Attribution
$\text{ZnL}^{2+} \cdot \text{H}_2\text{O}$ -S0	297	HOMO-4 \rightarrow LUMO 61%
	371	HOMO \rightarrow LUMO + 1 69%
$\text{ZnL}^{4+} \cdot \text{H}_2\text{O}$ -T0	415	HOMO \rightarrow LUMO 89%
	388	HOMO-6 \rightarrow LUMO + 1 35%
	393	HOMO-6 \rightarrow LUMO + 1 31%
$\text{ZnL}' \cdot \text{H}_2\text{O}$ -S1	480	HOMO \rightarrow LUMO 39%
	398	HOMO-1 \rightarrow LUMO 44%
		HOMO \rightarrow LUMO + 1 36%
$\text{ZnL}'^{2+} \cdot \text{H}_2\text{O}$ -S1	489	HOMO \rightarrow LUMO 87%
	410	HOMO-5 \rightarrow LUMO 89%
	490	HOMO \rightarrow LUMO + 1 57%

Table 2

Table 2. Relevant geometrical parameters (Å and °) of the compounds $\text{ZnL}^{2+} \cdot \text{H}_2\text{O}$ S0 and $\text{ZnL}^{4+} \cdot \text{H}_2\text{O}$ T0, optimized by the B3LYP/DZVP method, and of the compounds $\text{ZnL}' \cdot \text{H}_2\text{O}$ S1 and $\text{ZnL}'^{2+} \cdot \text{H}_2\text{O}$ S1, optimized by the CIS/DZVP method (see Fig. 1 for atom labels).

	$\text{ZnL}^{2+} \cdot \text{H}_2\text{O}$ -S0	$\text{ZnL}^{4+} \cdot \text{H}_2\text{O}$ -T0	$\text{ZnL}' \cdot \text{H}_2\text{O}$ -S1	$\text{ZnL}'^{2+} \cdot \text{H}_2\text{O}$ -S1
Zn-O1	1.994	2.043	1.985	1.985
Zn-O2	2.001	2.042	1.988	1.989
Zn-N1	2.117	2.113	2.124	2.153
Zn-N2	2.122	2.112	2.113	2.155
Zn-OH ₂	2.178	2.103	2.230	2.143
O1-Zn-O2	100.2	94.5	105.2	102.6
N1-Zn-N2	78.0	79.3	78.2	75.7
O1-Zn-N1	89.0	88.2	88.2	87.0
N1-Zn-O2	161.2	156.2	166.0	156.8

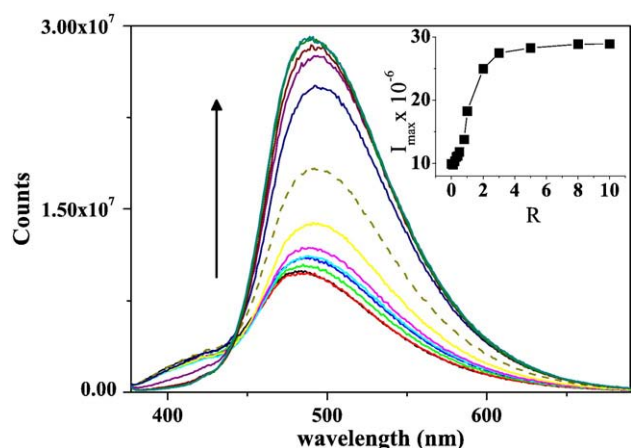


Fig. 10. Fluorescence spectra of solutions of the ZnL^{2+} complex, stored in the dark, in the presence of increasing amounts of DNA at fixed ZnL^{2+} concentration ($[\text{ZnL}^{2+}] = 5 \times 10^{-5} \text{ M}$), $R = 0.0$ (—), 0.10 (—), 0.20 (—), 0.30 (—), 0.40 (—), 0.50 (—), 0.80 (—), 1.0 (---), 2.0 (—), 3.0 (—), 5.0 (—), 8.0 (—); 10.0 (—) from the lowest to highest absorbance at 500 nm. In the inset the intensity (I_{max}) at the emission band maximum is reported as a function of R (line is only a guide for the eye).

concentration, the emission intensity at the band maximum is progressively enhanced reaching a plateau at $R \sim 3$ corresponding to a binding size of about 0.7 per base pairs which is in fair agreement with the literature value [22]. By plotting the fluorescence intensity at the band maximum as a function of R (inset in Fig. 10), it can be noted that a short induction regime (1) in the region $0 < R < 0.8$ was characterized by a nearly linear increase followed by a rapid increase (2) and finally a trend toward a plateau (3). This peculiar behavior reveals the existence of different binding regimes of ZnL^{2+} to the DNA double helix. It is worth to note that during phase (1), although the fraction of intercalated ZnL^{2+} is small, the DNA is completely saturated by ZnL^{2+} while the major part of the complex is in the aqueous medium or surrounding the DNA molecule. Accordingly, regime (1) could be attributed to the depletion of ZnL^{2+} -layers nearest the DNA surface [18]. Then, further increasing of the DNA concentration in the region $0.8 < R < 3$, together with an increase of the fraction of DNA-intercalated zinc(II) complex, the concentration of ZnL^{2+} outside tends to vanish. Finally, when the DNA concentration is very high all the ZnL^{2+} molecules are totally secluded within the DNA double helix. On the other hand, by considering the behavior of the wavelength at the maximum of the emission band (see Fig. 11), we observe a bathochromic shift in the $0 < R < 2$ range followed by a hypsochromic shift at $R > 2$. This finding indicates that this parameter monitors a different aspect of the intercalation process. Specifically, it is a fine probe of the environment experienced by ZnL^{2+} . The region where the bathochromic shift occurs corresponds to an increase of the fraction of the complex intercalated. On the other hand, the region of the hypsochromic shift reveals that, during the dilution process of ZnL^{2+} among the DNA binding sites, some changes of the DNA interior, involving an increase of its polarity, occur.

In order to estimate the environment sensed by the intercalated complex we have also collected its spectrum in methanol and ethanol. The comparison with that in aqueous solution is shown in Fig. 12. It can be noted that the wavelength at the band maximum in water (482 nm, dielectric constant 78) shifts at about 488 nm in methanol (dielectric constant 32.6) and at 510 nm in ethanol (dielectric constant 24.3). Considering that the highest value is observed in the presence of DNA (495 nm), it can be concluded that the intercalated complex probes an environment whose polarity is comprised between that of methanol and ethanol.

Further insights on the environment sensed by the intercalated complex were searched by monitoring the time-resolved fluorescence spectra of the complex in aqueous solution of native DNA. We have

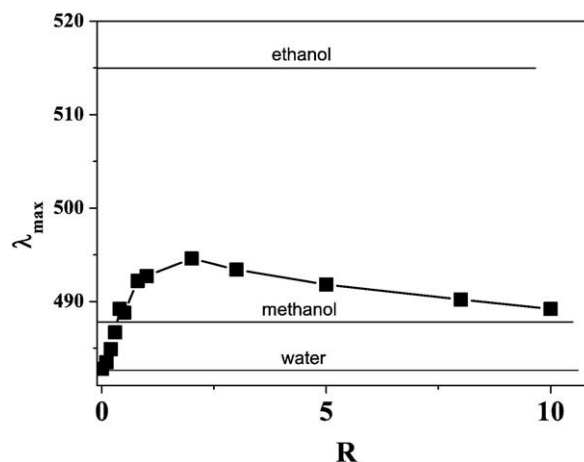


Fig. 11. Wavelength at the band maximum as a function of R (horizontal lines indicate the λ_{max} value of ZnL^{2+} in the specified solvent medium).

found that these spectra can be consistently described in terms of two exponential decay functions where, according to literature, the more fast decay characterized by a quite constant relaxation time of about 0.2 ns can be attributed to the sample scattering [48–50].

On the other hand, the second decay, attributable to the excited ZnL^{2+} complex, is characterized by a relaxation time which changes little going from the bulk aqueous phase (1.1 ns) to the DNA-intercalated state (0.9 ns). This piece of experimental result can be taken as an indication that the complex intercalation does not involve significant restriction of its molecular motions which should lead to a decrease of the nonradiative decay rate [51]. Moreover, the existence of a single decay time for the intercalated complex points toward the existence of nearly homogeneous binding sites.

5. Conclusions

The fluorescence intensity of the cationic Zn^{II} -5-triethyl ammonium methyl salicylidene ortho-phenylendiimine complex, ZnL^{2+} , in water solution at neutral pH, dramatically increases in the range 360–700 nm by exposure of the solution samples to tungsten light. Surprisingly, experimental results indicate that, in the intercalated state, ZnL^{2+} is effectively protected from this photochemical process. Quantum chemical calculations allowed us to suggest that in the free state ZnL^{2+} undergoes a photoinduced two-electron oxidation process and, consequently, the protective action of DNA toward the intercalated ZnL^{2+} can be attributed to an effective inhibition of the

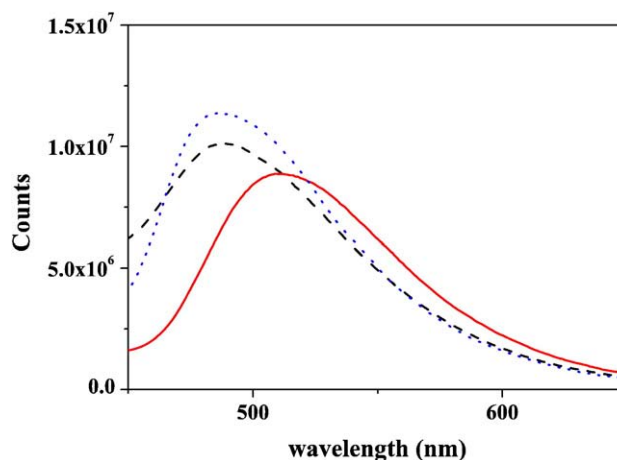


Fig. 12. Fluorescence spectra of ZnL^{2+} in water (---), methanol (···) and ethanol (—) at fixed concentration ($[\text{ZnL}^{2+}] = 5 \times 10^{-5} \text{ M}$).

ZnL²⁺ photooxidation. The latter conclusion is in agreement with the result that DNA-intercalated ZnL²⁺ is confined in a region less polar than water and inaccessible to this solvent, possibly being water the electron acceptor molecule of the ZnL²⁺ photooxidation.

Information achieved by steady state and time-resolved fluorescence spectroscopy indicates that the polarity of the environment probed by ZnL²⁺, intercalated within DNA, is comprised between that of methanol and ethanol and shows a continuous variation with the DNA to complex molar ratio. Indirectly, this finding allows to hypothesize that the structure of the DNA double helix progressively changes by increasing the fraction of occupied binding sites. From a more general prospect, the capability of DNA molecules to protect intercalated species from photodegradation processes seems to be of utmost importance from a biological point of view and could be amenable to biomedical applications.

Acknowledgements

Financial support from the Università di Palermo, Cariplo, and MIUR within the National Research Project “Dalle singole molecole a complessi e nanostrutture: struttura, chiralità, reattività e teoria” (PRIN 2006) is gratefully acknowledged. We thank also the “Fondazione Banco di Sicilia” (Palermo, Italy) for the co-funding of the Fluoromax 4 (Jobin Yvon) spectrofluorometer (Convenzione PR 19.b/06).

References

- [1] A. Rajendran, C.J. Magesh, P.T. Perumal, *Biochim. Biophys. Acta* 1780 (2008) 282–288.
- [2] A. Arola-Amal, J. Benet-Buchholz, S. Neidle, R. Vilar, *Inorg. Chem.* 47 (2008) (1919) 11910–11911.
- [3] B. Peng, W.-H. Zhou, L. Yan, H.-W. Liu, L. Zhu, *Trans. Met. Chem.* 34 (2009) 231–237.
- [4] K. Takahashi, K. Fukiura, H. Arai, M. Chikira, *Nucl. Acids Symp. Ser.* 51 (2007) 189–190.
- [5] G.-D. Liu, J.-P. Liao, S.-S. Huang, G.-L. Shen, R.-Q. Yu, *Anal. Sci.* 17 (2001) 1031–1036.
- [6] G.-D. Liu, X. Yang, Z.-P. Chen, G.-L. Shen, R.-Q. Yu, *Anal. Sci.* 16 (2000) 1255–1259.
- [7] D.J. Gravert, J.H. Griffin, *Inorg. Chem.* 35 (1996) 4837–4847.
- [8] K.I. Ansari, J.D. Grant, G.A. Woldemariam, S. Kasiri, S.S. Mandal, *Org. Biomol. Chem.* 7 (2009) 926–932.
- [9] G.A. Woldemariam, S.S. Mandal, *J. Inorg. Biochem.* 102 (2008) 740–747.
- [10] S. Bhattacharya, S.S. Mandal, *J. Chem. Soc. Chem. Commun.* (1995) 2489–2490.
- [11] J.G. Muller, L.A. Kayser, S.J. Paikoff, V. Duarte, N. Tang, R.J. Perez, S.E. Rokita, C.J. Burrows, *Coord. Chem. Rev.* 185–186 (1999) 761–774.
- [12] S. Routier, J.-L. Bernier, M.J. Waring, P. Colson, C. Houssier, C. Bailly, *J. Org. Chem.* 61 (1996) 2326–2331.
- [13] K. Sato, M. Chikira, Y. Fujii, A. Komatsu, *J. Chem. Soc. Chem. Commun.* (1994) 625–626.
- [14] G.B. Roy, *Inorg. Chim. Acta* 362 (2009) 1709–1714.
- [15] T. Kawasaki, T. Kamata, H. Ushijima, M. Kanakubo, S. Murata, F. Mizukami, Y. Fujii, Y. Usui, *J. Chem. Soc. Perkin Trans. 2* (1999) 193–198.
- [16] H. Kunkely, A. Vogler, *Inorg. Chim. Acta* 321 (2001) 171–174.
- [17] M.E. Germain, M.J. Knapp, *Inorg. Chem.* 47 (2008) 9748–9750.
- [18] K.E. Splan, A.M. Massari, G.A. Morris, S.-S. Sun, E. Reina, S.B.T. Nguyen, J.T. Hupp, *Eur. J. Inorg. Chem.* (2003) 2348–2351.
- [19] M.E. Germain, T.R. Vargo, P.G. Khalifah, M.J. Knapp, *Inorg. Chem.* 46 (2007) 4422–4429.
- [20] S.J. Wezenberg, E.C. Escudero-Adán, J. Benet-Buchholz, A.W. Kleij, *Org. Lett.* 10 (2008) 3311–3314.
- [21] G. Barone, N. Gambino, A. Ruggirello, A. Silvestri, A. Terenzi, V. Turco Liveri, *J. Inorg. Biochem.* 103 (2009) 731–737.
- [22] A. Silvestri, G. Barone, G. Ruisi, D. Anselmo, S. Riela, V. Turco Liveri, *J. Inorg. Biochem.* 101 (2007) 841–848.
- [23] G. Barone, A. Longo, A. Ruggirello, A. Silvestri, A. Terenzi, V. Turco Liveri, *Dalton Trans.* (2008) 4172–4178.
- [24] S.J. Angyal, P.J. Morris, J.R. Tetaz, J.G. Wilson, *J. Chem. Soc.* (1950) 2141–2145.
- [25] P. McPhie, *Methods Enzymol.* 22 (1971) 23–32.
- [26] S.D. Kennedy, R.G. Bryant, *Biophys. J.* 50 (1986) 669–676.
- [27] W.-K. Dong, Y.-X. Sun, Y.-P. Zhang, L. Li, X.-N. He, X.-L. Tang, *Inorg. Chim. Acta* 362 (2009) 117–124.
- [28] A.D. Becke, *J. Chem. Phys.* 98 (1993) 5648–5652.
- [29] N. Godbout, D.R. Salahub, J. Andzelm, E. Wimmer, *Can. J. Chem.* 70 (1992) 560–571.
- [30] C. Sosa, J. Andzelm, B.C. Elkin, E. Wimmer, K.D. Dobbs, D.A. Dixon, *J. Phys. Chem.* 96 (1992) 6630–6636.
- [31] E. Runge, E.K.U. Gross, *Phys. Rev. Lett.* 52 (1984) 997–1000.
- [32] R.E. Stratmann, G.E. Scuseria, M.J. Frisch, *J. Chem. Phys.* 109 (1998) 8218–8224.
- [33] R. Bauernschmitt, R. Ahlrichs, *Chem. Phys. Lett.* 256 (1996) 454–464.
- [34] M.E. Casida, C. Jamorski, K.C. Casida, D.R. Salahub, *J. Chem. Phys.* 108 (1998) 4439–4449.
- [35] J.B. Foresman, M. Head-Gordon, J.A. Pople, M.J. Frisch, *J. Phys. Chem.* 96 (1992) 135–149.
- [36] R.J. Cave, K. Burke, E.W. Castner Jr., *J. Phys. Chem. A* 106 (2002) 9294–9305.
- [37] D. Jacquemin, E.A. Perpète, G. Scalmani, M.J. Frisch, I. Ciofini, C. Adamo, *Chem. Phys. Lett.* 421 (2006) 272–276.
- [38] D. Jacquemin, E.A. Perpète, X. Assfeld, G. Scalmani, M.J. Frisch, C. Adamo, *Chem. Phys. Lett.* 438 (2007) 208–212.
- [39] V. Barone, M. Cossi, *J. Phys. Chem. A* 102 (1998) 1995–2001.
- [40] M.J. Frisch, G.W. Trucks, H.B. Schlegel, G.E. Scuseria, M.A. Robb, J.R. Cheeseman, J.A. Montgomery Jr., T. Vreven, K.N. Kudin, J.C. Burant, J.M. Millam, S.S. Iyengar, J. Tomasi, V. Barone, B. Mennucci, M. Cossi, G. Scalmani, N. Rega, G.A. Petersson, H. Nakatsuji, M. Hada, M. Ehara, K. Toyota, R. Fukuda, J. Hasegawa, M. Ishida, T. Nakajima, Y. Honda, O. Kitao, H. Nakai, M. Klene, X. Li, J.E. Knox, H.P. Hratchian, J.B. Cross, V. Bakken, C. Adamo, J. Jaramillo, R. Gomperts, R.E. Stratmann, O. Yazyev, A.J. Austin, R. Cammi, C. Pomelli, J.W. Ochterski, P.Y. Ayala, K. Morokuma, G.A. Voth, P. Salvador, J.J. Dannenberg, V.G. Zakrzewski, S. Dapprich, A.D. Daniels, M.C. Strain, O. Farkas, D.K. Malick, A.D. Rabuck, K. Raghavachari, J.B. Foresman, J.V. Ortiz, Q. Cui, A.G. Baboul, S. Clifford, J. Cioslowski, B.B. Stefanov, G. Liu, A. Liashenko, P. Piskorz, I. Komaromi, R.L. Martin, D.J. Fox, T. Keith, M.A. Al-Laham, C.Y. Peng, A. Nanayakkara, M. Challacombe, P.M.W. Gill, B. Johnson, W. Chen, M.W. Wong, C. Gonzalez, J.A. Pople, *Gaussian 03, Revision D.02*, Gaussian, Inc., Wallingford CT, 2005.
- [41] N.M. O'Boyle, A.L. Tenderholt, K.M. Langner, *J. Comput. Chem.* 29 (2008) 839–845, <http://gaussian.sourceforge.net>.
- [42] N.J. Turro, *Modern Molecular Photochemistry*, Benjamin-Cummings, Menlo Park, CA, 1978.
- [43] H. Kunkely, A. Vogler, *J. Photochem. Photobiol. A. Chem.* 138 (2001) 51–54.
- [44] H. Kunkely, A. Vogler, *Inorg. Chem. Commun.* 4 (2001) 692–694.
- [45] T. Fukuda, F. Sakamoto, M. Sato, Y. Nakano, X.S. Tana, Y. Fujii, *Chem. Commun.* (1998) 1391–1392.
- [46] W. Saenger, *Principles of Nucleic Acid Structure*, Springer Verlag, New York, 1984.
- [47] M. Raguz, J. Brnjas-Kraljevic, *J. Chem. Inf. Model.* 45 (2005) 1636–1640.
- [48] C.D. Byrne, A.J. de Mello, *Biophys. Chem.* 70 (1998) 173–184.
- [49] E.M. Talavera, P. Guerrero, F. Ocana, J.M. Alvarez-Pez, *Appl. Spectrosc.* 56 (2002) 80–87.
- [50] R.A. Hochstrasser, D.P. Millar, *Proceedings of SPIE, Int. Soc. Opt. Eng.* 1640 (1992) 599–605.
- [51] F. Ito, T. Kakiuchi, T. Nagamura, *J. Phys. Chem. C* 111 (2007) 6983–6988.